Quantum Criticality of Liquid-Gas Transition in a Binary Bose Mixture

Li He,[1,*] Haowei Li,[2,*] Wei Yi,[2,3] and Zeng-Qiang Yu[4,5,†]
[1]*College of Physics and Electronic Engineering, Shanxi University, Taiyuan 030006, China*
[2]*CAS Key Laboratory of Quantum Information, University of Science and Technology of China, Hefei 230026, China*
[3]*CAS Center For Excellence in Quantum Information and Quantum Physics, Hefei 230026, China*
[4]*Institute of Theoretical Physics, Shanxi University, Taiyuan 030006, China*
[5]*State Key Laboratory of Quantum Optics and Quantum Optics Devices, Shanxi University, Taiyuan 030006, China*

(Received 1 October 2022; revised 19 February 2023; accepted 17 April 2023; published 8 May 2023)

Quantum liquid, in the form of a self-bound droplet, is stabilized by a subtle balance between the mean-field contribution and quantum fluctuations. While a liquid-gas transition is expected when such a balance is broken, it remains elusive whether liquid-gas critical points exist in the quantum regime. Here, we study the quantum criticality in a binary Bose mixture undergoing the liquid-gas transition. We show that, beyond a narrow stability window of the self-bound liquid, a liquid-gas coexistence persists, which eventually transits into a homogeneous mixture. Importantly, we identify two distinct critical points where the liquid-gas coexistence terminates. These critical points are characterized by rich critical behaviors in their vicinity, including divergent susceptibility, unique phonon-mode softening, and enhanced density correlations. The liquid-gas transition and the critical points can be readily explored in ultracold atoms confined to a box potential. Our work highlights the thermodynamic approach as a powerful tool in revealing the quantum liquid-gas criticality, and paves the way for further studies of critical phenomena in quantum liquids.

DOI: 10.1103/PhysRevLett.130.193001

Introduction.—Liquid-gas transition is ubiquitous in nature, and serves as a paradigm of classical phase transitions. A well-known feature therein is the presence of critical points that mark the onset (or termination) of the liquid-gas coexistence [1]. In the quantum regime, exotic self-bound liquid states (dubbed quantum droplets) have recently been discovered in dipolar or binary Bose-Einstein condensates [2–12], and experimental observations consistent with the liquid-gas coexistence have been reported in imbalanced mixtures [9–12]. The discovery has stimulated extensive interest [13–52], culminating in the latest observation of dipolar supersolids in droplet crystals [53–58]. However, little is known about the transition between the inhomogeneous liquid-gas coexistence and the homogeneous liquid or gas phases, particularly in the thermodynamic limit. A further important question is whether there exists a quantum analog of the critical point in experimentally relevant systems. Since quantum fluctuations play a key role in the formation of self-bound droplets [2,15–18], they could lead to yet unexplored many-body phenomena at the critical points. A systematic investigation of such quantum criticality would therefore offer further insight into quantum liquids and enrich our understanding of quantum phase transitions in general.

In this Letter, we address the questions above by studying the liquid-gas transition in a three dimensional binary Bose mixture using a general thermodynamic approach. We find that, besides the self-bound state which is stable within a narrow window of densities [2], two types of liquid-gas coexistence generally exist, each with a distinct and fully polarized gas component (see Fig. 1). Upon further tuning the densities, the system undergoes a transition from a liquid-gas separated state to a homogeneous phase. Starting from the equation of state (EOS) with beyond-mean-field corrections, we quantitatively characterize the phase diagram in the thermodynamic limit, and, crucially, reveal two critical points where the liquid-gas coexistence terminates. Driven by density fluctuations, critical phenomena arise near the critical points, exemplified by the divergent susceptibility, the phonon-mode softening, and a dramatic enhancement of the correlation length. Given the recent progress in trapping and probing cold atoms, both the transition and quantum criticality reported here can be readily investigated in a box potential [59].

Liquid-gas coexistence.—We consider a three dimensional Bose mixture of cold atoms at zero temperature. The system features short-range interactions, with the interaction strengths g_{ij} ($i, j = 1, 2$ labeling the atomic species). Here, we consider interspecies attraction and intraspecies repulsion, with $g_{12} < 0$ and $g_{11}, g_{22} > 0$. On the mean-field level, the system would collapse when $g_{12} < -g$, with $g \equiv \sqrt{g_{11} g_{22}}$. Such instability, however, can be dramatically modified once the quantum fluctuations are taken into account [2]. We focus on the regime where $\delta\tilde{g} \equiv 1 + g_{12}/g$ is very small. It follows that, for a homonuclear mixture with equal masses ($m_1 = m_2 = m$), the energy per volume can be written as [2]

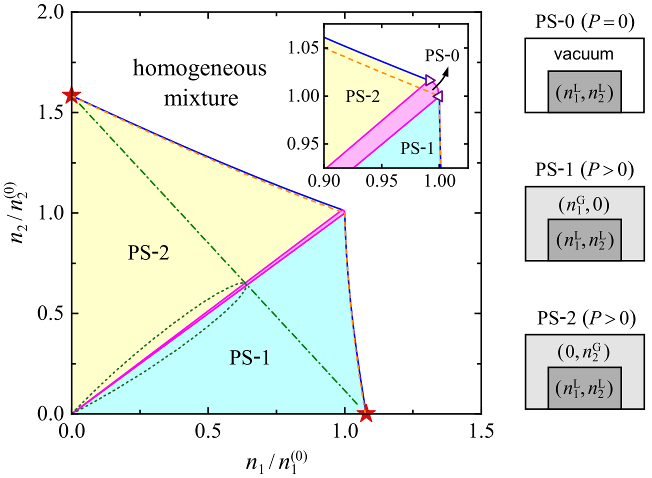

FIG. 1. Left: Ground-state phase diagram of a binary Bose mixture in the mean-field-unstable regime. The liquid-gas separated states PS-1 and PS-2 terminate at the critical points denoted by shaded star. Blue solid lines: phase boundaries obtained by numerically solving the balance conditions. Dashed lines: analytical boundaries given by Eq. (7) and its counterpart with an exchange of species index. The dash-dotted (dotted) line is the diffusive (mechanical) spinodal. Inset: enlarged view in the vicinity of $(n_1^{(0)}, n_2^{(0)})$. Leftward triangle (rightward triangle) denotes the point where the self-bound liquid reaches the evaporation threshold $\mu_1 = 0$ ($\mu_2 = 0$). Right: illustrations of various inhomogeneous states with either zero or positive pressure. For all figures throughout this Letter, $\delta\tilde{g} = -0.08$, and $\lambda = 0.68$, which are relevant for spin mixtures of ^{39}K atoms [8–10].

$$\mathcal{E} = \sum_{i,j=1,2} \frac{g_{ij}}{2} n_i n_j + \frac{8m^{3/2}}{15\pi^2\hbar^3}(g_{11}n_1 + g_{22}n_2)^{5/2}, \quad (1)$$

where n_1 and n_2 are the densities of the two species, respectively, $\hbar$ is the reduced Planck constant, and the second term represents the Lee-Huang-Yang corrections [60].

The EOS (1) is based on the presumption that the ground state is homogeneous. Yet, this is not true in the low-density limit under the mean-field instability. For a concentration n_1/n_2 fixed at $\lambda \equiv \sqrt{g_{22}/g_{11}}$, the attractive and the repulsive mean-field contributions are mostly canceled out, and the energy per particle reaches its minimum at the density [2]

$$n_i^{(0)} = \frac{25\pi}{1024a^3}\sqrt{\frac{g}{g_{ii}}}\frac{\lambda^{5/2}}{(1+\lambda)^5}\delta\tilde{g}^2, \quad (2)$$

with $a \equiv \sqrt{a_{11}a_{22}}$ ($a_{ij} = (mg_{ij}/4\pi\hbar^2)$ the s-wave scattering length). As a result, when the total atom density fulfills $n < n^{(0)}$, a self-bound liquid state is formed. Here, $n^{(0)} = n_1^{(0)} + n_2^{(0)}$. Such a state, referred to as PS-0 in Fig. 1, is stable even if the container of the system is removed, typical of the quantum droplet [8,9].

The realization of the quantum droplet is not restricted to the exact density ratio λ. Thermodynamically, a stable self-bound liquid can be achieved under the conditions [23,41]

$$P(n_1, n_2) = 0, \qquad \mu_1(n_1, n_2) \leqslant 0, \qquad \mu_2(n_1, n_2) \leqslant 0, \quad (3)$$

where P is the pressure, and μ_i is the chemical potential of species i. These conditions can be fulfilled within a narrow window of concentration, where the density of the self-bound liquid remains unchanged up to the order $\delta\tilde{g}^2$ [2].

If the population of species 1 increases further, such that the inequality $\mu_1 \leqslant 0$ no longer holds, the PS-0 state will evolve into an inhomogeneous state with liquid-gas coexistence (PS-1 in Fig. 1). The balance conditions for the phase separation are

$$P(n_1^L, n_2^L) = P(n_1^G, 0), \quad (4)$$

$$\mu_1(n_1^L, n_2^L) = \mu_1(n_1^G, 0), \quad (5)$$

$$\mu_2(n_1^L, n_2^L) < \mu_2(n_1^G, 0), \quad (6)$$

where n_1^L and n_2^L denote the densities of different species in the mixed liquid, and n_1^G is the density of the coexisting gas of species 1. While such liquid-gas coexistence has been numerically investigated in finite-size systems [33,50,52], the phase transition between the phase-separated state and a homogeneous one is not yet well understood.

Indeed, the PS-1 state appears only at sufficiently low densities, and the ground state becomes a homogeneous liquid under the conditions $n_i = n_i^L$. The coexistence boundary, in terms of n_1^L and n_2^L, can then be derived from Eqs. (4) and (5) by eliminating n_1^G. Keeping densities to the leading order in $\delta\tilde{g}^2$, we obtain the analytical form of the phase boundary [61]

$$\begin{aligned} 3(1+\lambda)^{5/2}(\tilde{n}_2^L)^2 - (\tilde{n}_1^L + \lambda\tilde{n}_2^L)^{3/2}[(5+3\lambda)\tilde{n}_2^L - 2\tilde{n}_1^L] \\ - 2(\tilde{n}_1^L - \tilde{n}_2^L)^{5/2} = 0, \end{aligned} \quad (7)$$

where $\tilde{n}_i^L = n_i^L/n_i^{(0)}$. As shown in Fig. 1, for small $\delta\tilde{g}$, the prediction of (7) is in good agreement with numerical calculations using Eqs. (4)–(6).

By tuning the density ratio, one can also realize another kind of liquid-gas coexistence, the PS-2 state, where the gas phase consists only of atoms of species 2. Its phase boundary can be readily obtained by enforcing $\tilde{n}_1^L \leftrightarrow \tilde{n}_2^L$ and $\lambda \to \lambda^{-1}$ in Eq. (7).

To shed more light on the phase-separated states, we introduce n_+ and n_- to discern what we call the hard and soft degrees of freedom in response to the density variation [2]

$$\begin{pmatrix} n_+ \\ n_- \end{pmatrix} = \begin{pmatrix} \cos\theta & -\sin\theta \\ \sin\theta & \cos\theta \end{pmatrix}\begin{pmatrix} n_1 \\ n_2 \end{pmatrix}, \quad (8)$$

with $\theta = \arctan \lambda$. A geometric interpretation of Eq. (8) can be clearly seen from the inset of Fig. 2. For a given n_+, the allowed values of n_- must be greater than the physical bound $n_-^{\min}$, where the system becomes a single-species gas. In the low-density regime, since $|\partial \mu_i / \partial n_+| \gg |\partial \mu_i / \partial n_-|$, the thermodynamic balance requires the hard-mode variable n_+ to be almost invariant in the coexisting phase (hence the name hard mode), enabling a single-mode approximation. As shown in Fig. 2, when n_+ lies within an appropriate range (expression given later), $\mathcal{E}(n_-)$ changes from concave to convex in the starting segment, meaning the energy of the phase-separated state (dashed lines) is lower than that of the homogenous state. Under the tangent Maxwell construction, the coexistence condition is thus

$$(n_-^L - n_-^{\min}) \frac{\partial \mathcal{E}}{\partial n_-}\bigg|_{n_-^L} = \mathcal{E}(n_+, n_-^L) - \mathcal{E}(n_+, n_-^{\min}). \tag{9}$$

For positive (negative) n_+, Eq. (9) gives the boundary of the PS-1 (PS-2) state, consistent with Eq. (7); for $n_+ = 0$, it recovers the zero-pressure condition for the self-bound liquid.

Using Eqs. (4) and (5), we have checked that the variation of n_+ in the coexisting liquid and gas phases vanishes at the order $\delta\tilde{g}^2$, which represents the accuracy of the single-mode approximation [61]. For a relatively larger $|\delta\tilde{g}|$, the terms neglected in the Lee-Huang-Yang contribution in Eq. (1) would result in a higher-order shift of the phase boundary.

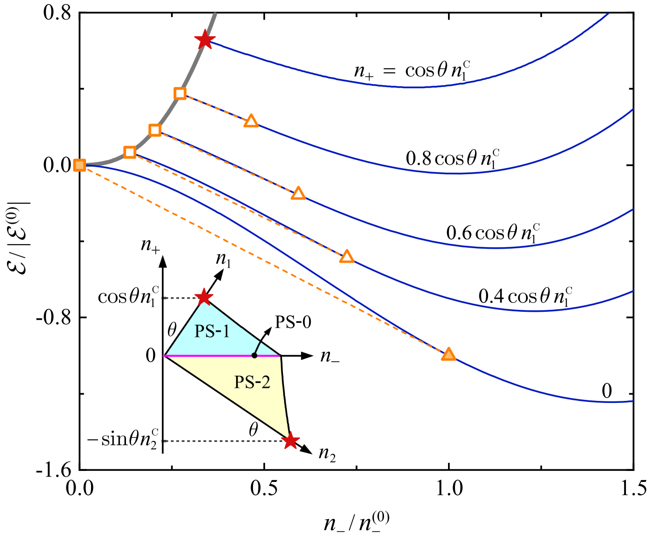

FIG. 2. EOS with the density variable n_+ fixed at different values. The dashed segments correspond to the energy of the inhomogeneous states. Orange square and orange triangle denote the coexisting liquid and gas phase, respectively. The filled symbols highlight the case of $n_+ = 0$, where the liquid is self-bound. The gray bold line represents the EOS of a pure gas of species 1. For a better view, $\mathcal{E}$ is shifted by $\frac{1}{2}(g_{11} + g_{22})n_+^2$. $\mathcal{E}^{(0)} = \frac{1}{3}(g + g_{12})n_1^{(0)} n_2^{(0)}$ is energy density of the self-bound liquid. The density variable n_- is measured in the unit of $n_-^{(0)} \equiv n_1^{(0)} \sin\theta + n_2^{(0)} \cos\theta$. Inset: phase diagram obtained in the single-mode approximation. Shaded star denotes the critical points.

Quantum criticality.—In part of the coexistence region, the homogeneous phase appears as a metastable state, similar to the superheated liquid in the classical liquid-gas transition [1]. When densities fall below the diffusive spinodal line fixed by $\gamma_1 \gamma_2 = \gamma_{12}^2$ ($\gamma_i \equiv (\partial \mu_i / \partial n_i)$ and $\gamma_{12} \equiv (\partial \mu_1 / \partial n_2)$), a homogeneous mixture becomes unstable against local density fluctuations. Note that the mechanical spinodal line, along which the compressibility diverges, lies inside the unstable region (see Fig. 1).

The diffusive spinodal line can be derived using the EOS (1), and corresponds to a straight line in the n_1-n_2 plane, satisfying $n_1/n_1^C + n_2/n_2^C = 1$ [61]. Since the spinodal must be enveloped by the coexistence boundaries, the difference between the separated phases vanishes at the densities $(n_1^C, 0)$ or $(0, n_2^C)$. In other words, the liquid-gas transitions terminate at these critical points. To the order $\delta\tilde{g}^2$, we find

$$n_i^C = \frac{16}{25}\left(1 + \frac{g}{g_{ii}}\right) n_i^{(0)}. \tag{10}$$

In the representation of (n_+, n_-), the liquid-gas coexistence only occurs within the interval $-\sin\theta n_2^C < n_+ < \cos\theta n_1^C$, while the homogeneous ground state evolves smoothly at either larger or smaller n_+, reminiscent of the supercritical regime of a classical liquid-gas transition.

Importantly, in the vicinity of these critical points, density fluctuations dominate and give rise to abundant critical behaviors. Thermodynamically, the quantum criticality is manifested in the singular behavior of the susceptibilities $\chi_{ij}^0 \equiv (\partial n_i / \partial \mu_j)_{\mu_{3-j}}$, which characterize the static response to density perturbations. With some algebra, χ_{ij}^0 can be rewritten as

$$\chi_{ii}^0 = \frac{\gamma_{3-i}}{\gamma_1 \gamma_2 - \gamma_{12}^2}, \qquad \chi_{12}^0 = \chi_{21}^0 = \frac{-\gamma_{12}}{\gamma_1 \gamma_2 - \gamma_{12}^2}, \tag{11}$$

which become divergent at either critical point.

Another related critical phenomenon is the softening of the phonon excitations. Specifically, we derive the sound velocities of the phonon modes using the standard hydrodynamic approach [61]

$$c_\pm = \sqrt{\frac{1}{2m}\left[\gamma_1 n_1 + \gamma_2 n_2 \pm \sqrt{(\gamma_1 n_1 - \gamma_2 n_2)^2 + 4\gamma_{12}^2 n_1 n_2}\right]}, \tag{12}$$

where c_- vanishes at either critical point. At first glance, this seems quite natural, since only one phonon mode can survive as the density of the minority species approaches zero. However, it is only at the critical points that c_- exhibits a unique linear dependence on the vanishing minority density. For instance, in the low-concentration limit with $n_1 = n_1^C$, the sound velocity $c_- = (5\sqrt{\lambda}/2\sqrt{2})c_-^{(0)}\tilde{n}_2$, where $\tilde{n}_2 = n_2/n_2^{(0)}$, and $c_-^{(0)} = 4\sqrt{gn^{(0)}\sqrt{n^{(0)}a^3}/5\sqrt{\pi}m}$ is the sound velocity of the self-bound liquid [61]. In contrast, we find $c_- \propto \sqrt{\tilde{n}_2}$ in the low-concentration limit with a fixed $n_1 > n_1^C$. Such distinction [see Fig. 3(a)] provides a clear signature for detecting the critical points. Note that, for $n_1 < n_1^C$, c_- becomes imaginary in the spinodal region, indicating a dynamic instability.

The quantum criticality is also manifested in the dramatic changes in the correlation length. The relative probability of finding two particles of a given species at distance r is measured by the pair-distribution function $\mathcal{D}_{ij}(r)$, which at large separation takes the form $\mathcal{D}_{ij}(r \to \infty) = 1 - (\xi_{ij}/\sqrt{2n_i n_j}\pi^2 r^4)$, with ξ_{ij} the correlation length [67,68]. Thus, the combined length scale $(\xi_{ij}/\sqrt{n_i n_j})^{1/4}$ represents a characteristic distance, over which $\mathcal{D}_{ij}$ deviates considerably from unity. To determine ξ_{ij}, we employ the hydrodynamic approach to derive the dynamic density response function, which is connected to the Fourier transform of $\mathcal{D}_{ij}$ through the fluctuation-dissipation theorem. ξ_{ij} is then extracted from the asymptotic expansion of $\mathcal{D}_{ij}$ [61].

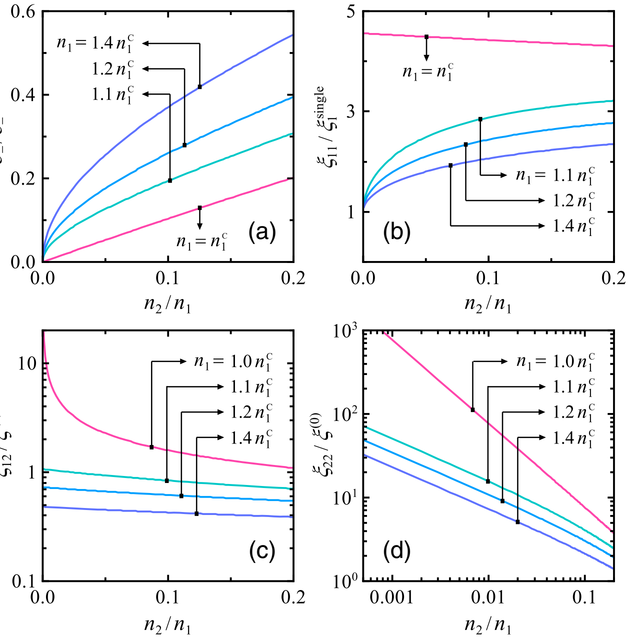

FIG. 3. (a) Sound velocity c_- and (b–d) correlation lengths ξ_{ij} as functions of the minority concentration n_2/n_1, for different n_1.

At a critical point, for instance $n_1 = n_1^C$ and $n_2 \to 0$, ξ_{ij} behaves like [61]

$$\xi_{11} \to \xi_1^{\text{single}}\left(1 + \frac{1}{\sqrt{|\delta\tilde{g}|}}\right), \tag{13}$$

$$\xi_{12} \sim \frac{\xi^{(0)}}{\sqrt{\tilde{n}_2}} \to \infty, \qquad \xi_{22} \sim \frac{\xi^{(0)}}{\tilde{n}_2} \to \infty, \tag{14}$$

where $\xi_1^{\text{single}} = \hbar/\sqrt{2mn_1\gamma_1}|_{n_2=0}$ is the healing length of a single-species Bose gas [67,69], $\xi^{(0)} = [\sqrt{3}\hbar(\sqrt{g_{11}} + \sqrt{g_{22}})/g\sqrt{2m|\delta\tilde{g}|n^{(0)}}]$ is the typical surface thickness of a self-bound droplet [2]. By contrast, for the case with any given $n_1 > n_1^C$ (and $n_2 \to 0$), we have [61]

$$\xi_{11} \to \xi_1^{\text{single}}, \qquad \xi_{12} \to A\xi^{(0)}, \qquad \xi_{22} \sim \frac{\xi^{(0)}}{\sqrt{\tilde{n}_2}} \to \infty, \tag{15}$$

with the coefficient A given in Supplemental Material [61]. The distinction between these two situations, as illustrated in Figs. 3(b)–3(d), reflects the significant enhancement of density correlations at the quantum criticality, and can be tested experimentally using the Bragg spectroscopy. Note that the discussions above apply to the other critical point by exchanging the species labels.

It is worth noting that the structures of the PS-1 and PS-2 states resemble that of the partially miscible states recently predicted for $g_{12} > g$ [70], where the Lee-Huang-Yang correction also plays a crucial role in establishing the coexistence equilibrium. The key difference is that, under the repulsive interspecies interactions in Ref. [70], the phase separation occurs between gaseous phases and the dynamic instability is due to the out-of-phase fluctuations of two species; whereas in our case ($g_{12} < -g$), the underlying quantum criticality originates from the in-phase fluctuations.

Density profiles.—The predicted phase diagram can be experimentally verified with ultracold atoms confined in a box potential [59]. We numerically simulate the atomic density profiles by solving the extended Gross-Pitaevskii equation [2]

$$\left[-\frac{\hbar^2\nabla^2}{2m} + \frac{\partial}{\partial n_i}\mathcal{E}[n_1(\mathbf{r}), n_2(\mathbf{r})] - \bar{\mu}_i^{\text{box}}\right]\psi_i(\mathbf{r}) = 0, \tag{16}$$

where ψ_i is the condensate wave function satisfying the boundary condition $\psi_i = 0$ at hard walls of the box, and $\bar{\mu}_i^{\text{box}}$ is the global chemical potential fixed by the normalization condition $\int d\mathbf{r}|\psi_i(\mathbf{r})|^2 = N_i$. For simplicity, we consider a spherical box trap of radius R_{box}, and introduce dimensionless variables $\tilde{N}_i = N_i/n_i^{(0)}\xi^{(0)3}$ and $\tilde{V}_{\text{box}} = (R_{\text{box}}/\xi^{(0)})^3$. The ground state of the system is numerically determined through imaginary-time evolutions under the split-step method [71].

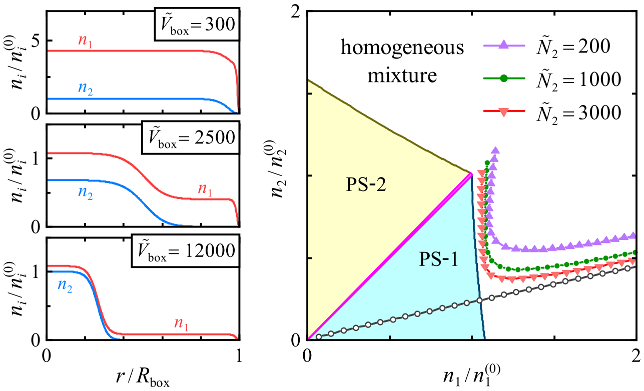

FIG. 4. Left: atomic density profiles in a box trap of different sizes with $(\tilde{N}_1, \tilde{N}_2) = (5000, 1000)$. Right: trajectory of the central density during an adiabatic expansion with various atom numbers. For comparison, the result for the case with $\delta\tilde{g} = 0$ and $\tilde{N}_2 = 3000$ is also shown (circle). All the simulations are performed with the concentration $\tilde{N}_1/\tilde{N}_2 = 5$.

As illustrated in the left column of Fig. 4, for sufficiently small $\tilde{V}_{\rm box}$, the atomic densities are almost uniform, except for a thin layer close to the boundary. When $\tilde{V}_{\rm box}$ increases beyond a certain threshold, the liquid-gas coexistence appears, and the density profile exhibits a shell structure, with a liquid core immersed in a single-component gas of the majority species. Here, the densities of the two coexisting phases roughly obey the relation $\tilde{n}_1^G = \tilde{n}_1^L - \tilde{n}_2^L$ with $\tilde{n}_i^G = n_i^G/n_i^{(0)}$, consistent with results from the single-mode approximation. As $\tilde{V}_{\rm box}$ further increases, the gas in the outer shell becomes extremely dilute, and the liquid core is essentially self-bound with the densities approaching the saturated values $(n_1^{(0)}, n_2^{(0)})$. These results imply that, under the liquid-gas coexistence, a clear distinction between the gas and the liquid phases can be observed during an adiabatic expansion—while the outer gas shell diffuses throughout the box, the liquid core retains a finite volume.

Further, the phase diagram can be readily extracted from the flattop density profile. The right panel of Fig. 4 shows the evolution of the central density when $\tilde{V}_{\rm box}$ gradually increases at a fixed concentration $\tilde{N}_1/\tilde{N}_2 = 5$. As the phase separation sets in, the density trajectory turns upward abruptly and follows the phase boundary of the PS-1 state. Such a behavior is in stark contrast to the case without a liquid-gas transition (empty circles). By choosing a concentration $\tilde{N}_1/\tilde{N}_2 \ll 1$, the boundary of PS-2 state can also be obtained.

Because of the finite-size effect, the phase boundary constructed in this way shows some deviations from that in the thermodynamic limit. The deviation becomes less pronounced when $\tilde{N}_i \gtrsim 1000$ (see Fig. 4). Under our choice of parameters (see Fig. 1), the condition $(\tilde{N}_1, \tilde{N}_2) = (1, 1)$ corresponds to $(N_1, N_2) = (1.16, 1.71) \times 10^3$, which means that experiments with atom numbers of the order 10^6 should suffice.

Discussion.—Adopting a thermodynamic approach, we quantitatively characterize the liquid-gas coexistence in a mean-field-unstable Bose mixture, and reveal the underlying quantum criticality. The liquid-gas transition considered here also occurs in heteronuclear mixtures such as ^{41}K-^{87}Rb [11] and ^{23}Na-^{87}Rb [12], where similar phase diagrams can be established using the analytical EOS therein [61,70].

For future studies, it is desirable to explore the quantum liquid-gas criticality in lower dimensions [14,25,26,30,35,42], with three-body [72,73] or dipolar [3–7,15–17,20,43,44,53–58] interactions, or at finite temperatures [39,40,46–48]. At finite temperatures in particular, the interplay between quantum and thermal fluctuations may affect the nature of the condensation [39,48,74], giving rise to intriguing critical behaviors.

We thank Lan Yin and Shizhong Zhang for helpful discussions. This research is supported by NSFC under Grants No. 12174230 and No. 12147215 (Z.-Q. Y.), Grant No. 12104275 (L. H.), and Grant No. 11974331 (W. Y.); and partially by the Fund for Shanxi 1331 Project of Key Subjects Construction.

Note added.—Recently, we became aware of a related work [75], where the liquid-gas transition and the associated critical behavior are discussed in a different setup.

---

[*] These authors contributed equally to this work.

[†] zqyu.physics@outlook.com

[1] L. D. Landau and E. M. Lifshitz, *Statistical Physics*, Part 1 (Pergamon Press, New York, 1980).
[2] D. S. Petrov, Phys. Rev. Lett. **115**, 155302 (2015).
[3] H. Kadau, M. Schmitt, M. Wenzel, C. Wink, T. Maier, I. Ferrier-Barbut, and T. Pfau, Nature (London) **530**, 194 (2016).
[4] I. Ferrier-Barbut, H. Kadau, M. Schmitt, M. Wenzel, and T. Pfau, Phys. Rev. Lett. **116**, 215301 (2016).
[5] M. Schmitt, M. Wenzel, F. Böttcher, I. Ferrier-Barbut, and T. Pfau, Nature (London) **539**, 259 (2016).
[6] L. Chomaz, S. Baier, D. Petter, M. J. Mark, F. Wächtler, L. Santos, and F. Ferlaino, Phys. Rev. X **6**, 041039 (2016).
[7] F. Böttcher, M. Wenzel, J.-N. Schmidt, M. Guo, T. Langen, I. Ferrier-Barbut, T. Pfau, R. Bombín, J. Sánchez-Baena, J. Boronat, and F. Mazzanti, Phys. Rev. Res. **1**, 033088 (2019).
[8] C. Cabrera, L. Tanzi, J. Sanz, B. Naylor, P. Thomas, P. Cheiney, and L. Tarruell, Science **359**, 301 (2018).
[9] G. Semeghini, G. Ferioli, L. Masi, C. Mazzinghi, L. Wolswijk, F. Minardi, M. Modugno, G. Modugno, M. Inguscio, and M. Fattori, Phys. Rev. Lett. **120**, 235301 (2018).
[10] P. Cheiney, C. R. Cabrera, J. Sanz, B. Naylor, L. Tanzi, and L. Tarruell, Phys. Rev. Lett. **120**, 135301 (2018).

[11] C. D'Errico, A. Burchianti, M. Prevedelli, L. Salasnich, F. Ancilotto, M. Modugno, F. Minardi, and C. Fort, Phys. Rev. Res. **1**, 033155 (2019).
[12] Z. Guo, F. Jia, L. Li, Y. Ma, J. M. Hutson, X. Cui, and D. Wang, Phys. Rev. Res. **3**, 033247 (2021).
[13] For reviews, see F. Böttcher, J.-N. Schmidt, J. Hertkorn, K. S. H. Ng, S. D. Graham, M. Guo, T. Langen, and T. Pfau, Rep. Prog. Phys. **84**, 012403 (2021); Z.-H. Luo, W. Pang, B. Liu, Y.-Y. Li, and B. A. Malomed, Front. Phys. **16**, 32201 (2021).
[14] D. S. Petrov and G. E. Astrakharchik, Phys. Rev. Lett. **117**, 100401 (2016).
[15] F. Wächtler and L. Santos, Phys. Rev. A **93**, 061603(R) (2016).
[16] R. N. Bisset, R. M. Wilson, D. Baillie, and P. B. Blakie, Phys. Rev. A **94**, 033619 (2016).
[17] F. Wächtler and L. Santos, Phys. Rev. A **94**, 043618 (2016).
[18] M. Wenzel, F. Böttcher, T. Langen, I. Ferrier-Barbut, and T. Pfau, Phys. Rev. A **96**, 053630 (2017).
[19] A. Cappellaro, T. Macri, G. F. Bertacco, and L. Salasnich, Sci. Rep. **7**, 13358 (2017).
[20] D. Baillie and P. B. Blakie, Phys. Rev. Lett. **121**, 195301 (2018).
[21] C. Staudinger, F. Mazzanti, and R. E. Zillich, Phys. Rev. A **98**, 023633 (2018).
[22] V. Cikojević, K. Dželalija, P. Stipanović, L. Vranješ Markić, and J. Boronat, Phys. Rev. B **97**, 140502(R) (2018).
[23] F. Ancilotto, M. Barranco, M. Guilleumas, and M. Pi, Phys. Rev. A **98**, 053623 (2018).
[24] E. Chiquillo, Phys. Rev. A **97**, 063605 (2018).
[25] P. Zin, M. Pylak, T. Wasak, M. Gajda, and Z. Idziaszek, Phys. Rev. A **98**, 051603(R) (2018).
[26] T. Ilg, J. Kumlin, L. Santos, D. S. Petrov, and H. P. Büchler, Phys. Rev. A **98**, 051604(R) (2018).
[27] N. B. Jørgensen, G. M. Bruun, and J. J. Arlt, Phys. Rev. Lett. **121**, 173403 (2018).
[28] G. Ferioli, G. Semeghini, L. Masi, G. Giusti, G. Modugno, M. Inguscio, A. Gallemí, A. Recati, and M. Fattori, Phys. Rev. Lett. **122**, 090401 (2019).
[29] V. Cikojević, L. V. Markić, G. E. Astrakharchik, and J. Boronat, Phys. Rev. A **99**, 023618 (2019).
[30] L. Parisi, G. E. Astrakharchik, and S. Giorgini, Phys. Rev. Lett. **122**, 105302 (2019).
[31] F. Minardi, F. Ancilotto, A. Burchianti, C. D'Errico, C. Fort, and M. Modugno, Phys. Rev. A **100**, 063636 (2019).
[32] G. Ferioli, G. Semeghini, S. Terradas-Briansó, L. Masi, M. Fattori, and M. Modugno, Phys. Rev. Res. **2**, 013269 (2020).
[33] T. Mithun, A. Maluckov, K. Kasamatsu, B. A. Malomed, and A. Khare, Symmetry **12**, 174 (2020).
[34] H. Hu and X.-J. Liu, Phys. Rev. Lett. **125**, 195302 (2020).
[35] H. Hu, J. Wang, and X.-J. Liu, Phys. Rev. A **102**, 043301 (2020).
[36] H. Hu and X.-J. Liu, Phys. Rev. A **102**, 053303 (2020).
[37] Y. Wang, L. Guo, S. Yi, and T. Shi, Phys. Rev. Res. **2**, 043074 (2020).
[38] Q. Gu and L. Yin, Phys. Rev. B **102**, 220503(R) (2020).
[39] L. He, P. Gao, and Z.-Q. Yu, Phys. Rev. Lett. **125**, 055301 (2020).
[40] J. Wang, X.-J. Liu, and H. Hu, Chin. Phys. B **30**, 010306 (2021).
[41] P. Zin, M. Pylak, and M. Gajda, Phys. Rev. A **103**, 013312 (2021).
[42] L. Lavoine and T. Bourdel, Phys. Rev. A **103**, 033312 (2021).
[43] R. N. Bisset, L. A. Peña Ardila, and L. Santos, Phys. Rev. Lett. **126**, 025301 (2021).
[44] Joseph C. Smith, D. Baillie, and P. B. Blakie, Phys. Rev. Lett. **126**, 025302 (2021).
[45] T. G. Skov, M. G. Skou, N. B. Jørgensen, and J. J. Arlt, Phys. Rev. Lett. **126**, 230404 (2021).
[46] G. De Rosi, G. E. Astrakharchik, and P. Massignan, Phys. Rev. A **103**, 043316 (2021).
[47] N. Guebli and A. Boudjemâa, Phys. Rev. A **104**, 023310 (2021).
[48] H. Hu, Z.-Q. Yu, J. Wang, and X.-J. Liu, Phys. Rev. A **104**, 043301 (2021).
[49] V. Cikojević, E. Poli, F. Ancilotto, L. Vranješ-Markić, and J. Boronat, Phys. Rev. A **104**, 033319 (2021).
[50] M. N. Tengstrand and S. M. Reimann, Phys. Rev. A **105**, 033319 (2022).
[51] Y. Xiong and L. Yin, Phys. Rev. A **105**, 053305 (2022).
[52] T. A. Flynn, L. Parisi, T. P. Billam, and N. G. Parker, arXiv:2209.04318.
[53] L. Tanzi, E. Lucioni, F. Famà, J. Catani, A. Fioretti, C. Gabbanini, R. N. Bisset, L. Santos, and G. Modugno, Phys. Rev. Lett. **122**, 130405 (2019).
[54] F. Böttcher, J.-N. Schmidt, M. Wenzel, J. Hertkorn, M. Guo, T. Langen, and T. Pfau, Phys. Rev. X **9**, 011051 (2019).
[55] L. Chomaz, D. Petter, P. Ilzhöfer, G. Natale, A. Trautmann, C. Politi, G. Durastante, R. M. W. van Bijnen, A. Patscheider, M. Sohmen, M. J. Mark, and F. Ferlaino, Phys. Rev. X **9**, 021012 (2019).
[56] G. Natale, R. M. W. van Bijnen, A. Patscheider, D. Petter, M. J. Mark, L. Chomaz, and F. Ferlaino, Phys. Rev. Lett. **123**, 050402 (2019).
[57] L. Tanzi, S. M. Roccuzzo, E. Lucioni, F. Famà, A. Fioretti, C. Gabbanini, G. Modugno, A. Recati, and S. Stringari, Nature (London) **574**, 382 (2019).
[58] M. Guo, F. Böttcher, J. Hertkorn, J.-N. Schmidt, M. Wenzel, H. P. Büchler, T. Langen, and T. Pfau, Nature (London) **574**, 386 (2019).
[59] N. Navon, R. P. Smith, and Z. Hadzibabic, Nat. Phys. **17**, 1334 (2021).
[60] T. D. Lee, K. Huang, and C. N. Yang, Phys. Rev. **105**, 1119 (1957).
[61] See Supplemental Material at http://link.aps.org/supplemental/10.1103/PhysRevLett.130.193001 for details on the derivation of the phase boundaries, the hydrodynamic approach, and the critical phenomena, where Refs. [62–66] are included.
[62] K. Huang, *Statistical Mechanics* (John Wiley & Sons, New York, 1987).
[63] C. Pethick and H. Smith, *Bose-Einstein Condensation in Dilute Gases* (Cambridge University Press, New York, 2008).
[64] J. Nespolo, G. E. Astrakharchik, and A. Recati, New J. Phys. **19**, 125005 (2017).
[65] D. Romito, C. Lobo, and A. Recati, Phys. Rev. Res. **3**, 023196 (2021).

[66] M. J. Lighthill, *An Introduction to Fourier Analysis and Generalized Functions* (Cambridge University Press, London, 1958).

[67] T. D. Lee, K. Huang, and C. N. Yang, Phys. Rev. **106**, 1135 (1957).

[68] E. Feenberg, *Theory of Quantum Fluids* (Academic Press, New York, 1969).

[69] L. P. Pitaevskii and S. Stringari, *Bose-Einstein Condensation and Superfluidity* (Oxford University Press, New York, 2016).

[70] P. Naidon and D. S. Petrov, Phys. Rev. Lett. **126**, 115301 (2021).

[71] J. Javanainen and J. Ruostekoski, J. Phys. A **39**, L179 (2006).

[72] A. Gammal, T. Frederico, L. Tomio, and Ph. Chomaz, Phys. Rev. A **61**, 051602(R) (2000).

[73] A. Bulgac, Phys. Rev. Lett. **89**, 050402 (2002).

[74] D. T. Son, M. Stephanov, and H. U. Yee, J. Stat. Mech. (2021) 013105.

[75] Q. Gu and X. Cui, Phys. Rev. A **107**, L031303 (2023).